Endowing catanionic surfactant vesicles with dual responsive abilities *via* a noncovalent strategy: introduction of a responser, sodium cholate†

Lingxiang Jiang, Ke Wang, Fuyou Ke, Dehai Liang and Jianbin Huang*

Received 4th August 2008, Accepted 22nd October 2008
First published as an Advance Article on the web 1st December 2008
DOI: 10.1039/b813498g

A noncovalent strategy is proposed for endowing responseless catanionic surfactant (a mixture of cationic and anionic surfactants) aggregates with responsive abilities by addition of a responser. In this strategy, the composition of catanionic surfactant can be carefully selected to render aggregates sensitive to added responsers, and the responsers can be chosen from plenty of commercialized candidates, which bear responsive groups and will be noncovalently incorporated into the aggregates. In this paper, we report an illustrative example for the strategy: dual-responsive vesicles are realized by simply adding a responser, SC (sodium cholate), to a stimuli-inert DEAB/SDS (dodecyl triethyl ammonium bromide/sodium dodecyl sulfate) vesicular aqueous solution at a low responser/surfactant molar ratio of 0.045. The resultant DEAB/SDS/SC aggregates undergo reversible transitions between vesicles and micelles in response to temperature or pH variations. Possible mechanisms for these responsive behaviors are speculated, where the temperature-responsive hydroxyl groups and pH-responsive carboxylate group of SC are thought to be crucial. This responsive ability-endowing noncovalent strategy shows potential as a general, versatile, and economical method for fabricating stimuli-responsive self-assemblies.

Introduction

Responsive vesicles

Vesicles are indispensable self-assembled aggregates for *in vitro* studies because they afford geometrically restricted systems to reproduce cell organizations, are capable of encapsulating peptides, nucleic acids, or drugs in their inner water pools, and can protect labile substances against degradation by their semi-permeable membranes.[1–3] In particular, aggregate transitions between vesicles and micelles are of great importance. The micelle-to-vesicle transition (MVT) is an advantageous method for loading substances and a critical step in reconstituting membrane proteins into vesicle membranes that provide a biomimetic environment. Its reverse process, the vesicle-to-micelle transition (VMT), is closely related to the isolation and purification of membrane proteins, as well as to the release of encapsulated substances.[4–7]

Recently, there has been an increasing demand for controlling or manipulating the structure and properties of aggregates including vesicles, which has been partially met by "smart" stimuli-responsive aggregates.[8–10] Indeed, responsive vesicles are superior to conventional vesicles and show great potential in drug/gene delivery or protein reconstitutions.[11–13] So far, they have been achieved by functionalizing amphiphiles in which responsive moieties, such as amines, ferrocene, azobenzenes, and amylases, are covalently incorporated.[12–20] However, most of the functionalized molecules require laborious, multi-step, or even low-yield syntheses, and their resultant vesicles only respond to one stimulus. To sidestep these difficult syntheses and endow vesicles with multi-responsive abilities, an alternative noncovalent strategy is proposed in this paper.

Design of the noncovalent strategy

In this strategy, we attempt to fabricate responsive vesicles by simply mixing two components in a solution: the major one is vesicle-forming, the minor one is stimuli-responsive (a responser), and they can noncovalently self-assemble. Several precedents have tested the basic principle of the strategy: liposomes can become sensitive to pH,[21] redox,[22] or transition metal ions[23,24] by doping with specific additives; liposome formation can be induced by enzymes[25] or temperature jumps[26] in lipid/detergent mixtures; cationic surfactant worm-like micelles can respond to temperature[27,28] or light[29] by mixing with hydrotropes. However, these cases appear to suffer from the difficulty that the aggregates are not significantly affected by the added responsers (*i.e.*, they are insensitive to the responsers), which is compensated by complicated design and syntheses of the specific additives or by high concentrations of the added detergents or hydrotropes. To overcome this difficulty, catanionic surfactant systems (aqueous mixtures of a cationic and an anionic surfactant) might provide an alternative.

Catanionic surfactant systems[30–32] exhibit a broad range of aggregate morphologies, including micelles, vesicles, lamellae, tubes, and regular hollow icosahedra.[33–39] Transitions between

Beijing National Laboratory for Molecular Sciences (BNLMS), College of Chemistry and Molecular Engineering, Peking University, Beijing, 100871, China. E-mail: jbhuang@pku.edu.cn; Fax: +86-10-62751708; Tel: +86-10-62753557

† Electronic supplementary information (ESI) available: Fig. S1 to S4. See DOI: 10.1039/b813498g

these aggregate morphologies are mainly dependent on the surfactant composition: for example, micelles, vesicles, and precipitates are generally formed when surfactant compositions are greatly different from, close to, and exactly at equimolarity (*i.e.*, electroneutral mixing), respectively. By carefully choosing a composition that is within a vesicular region and near a vesicle/micelle boundary, one can obtain vesicles that are ready to be transformed into micelles. The high sensitivity of catanionic surfactant vesicles to additives was confirmed by our previous work.[40–42] According to this viewpoint, addition of a responser to these vesicles is expected to bring them pronounced responsive abilities. In addition, catanionic surfactant vesicles possess other advantages, such as the commercial availability of their components, spontaneous formation, and long-term stability.[30]

After obtaining responser-sensitive catanionic surfactant vesicles, one can relatively easily choose a responser from abundant commercial available candidates, which bear desirable responsive groups and are somewhat hydrophobic in nature. This hydrophobic nature drives the response into aggregates through the hydrophobic effect. To this end, we selected SC (sodium cholate) as the responser, which has three temperature-responsive hydroxyl groups, a pH-responsive carboxylate group, and a hydrophobic steroid skeleton (Fig. 1). SC is a member of the bile salts, which are different from conventional "head-and-tail" surfactants and are well-known as facial amphiphiles composed of a rigid steroid skeleton, a polar face, and a nonpolar face.[43–45] Specifically, dual-responsive vesicles are obtained by adding a low amount of SC to a responseless DEAB/SDS (dodecyl triethyl ammonium bromide/sodium dodecyl sulfate) vesicular aqueous solution. In the resulting DEAB/SDS/SC solution, micelles are major aggregates at 25 °C and pH 6.8, whereas vesicles are major aggregates at 60 °C or pH 3.4. That is to say, the MVT occurs with heating or acidifying, while the VMT comes about with cooling or alkalifying. As to the origin of the aggregate transitions, the hydroxyl and carboxylate groups of SC may be responsible.

Experimental section

Materials

Dodecyl triethyl ammonium bromide (DEAB), dodecyl trimethyl ammonium bromide (DTAB), dodecyltripropyl ammonium bromide (DPAB), and dodecyl diethyl methyl ammonium bromide (DE_2MAB) were prepared by reactions of 1-bromododecane with corresponding amines, followed by recrystallizing five times from ethanol–acetone. Sodium dodecyl sulfate (SDS, Acros), sodium dodecyl benzene sulfonate (SDBS, Acros), sodium cholate (SC, Fluka), Triton X-100 (Merck), and $C_{12}EO_{10}$ (Merck) were used as received. The purities of the surfactants were examined by the lack of minimum in their surface tension curves. The water used was re-distilled from potassium permanganate. The other reagents were of A. R. grade.

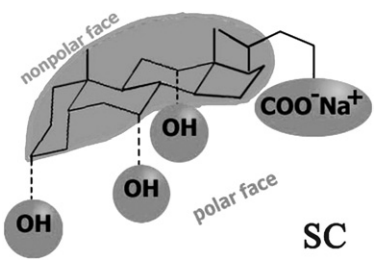

Fig. 1 Molecular structure of SC. Its facially amphiphilic structure is highlighted. Its hydroxyl groups and carboxylate group are sensitive to temperature and pH, respectively. This representation follows ref. 45.

Absorbance measurements

Absorbance measurements were carried out at 500 nm with a Beijing Purkinje General TU-1810 spectrophotometer, which was controlled at the desired temperature.

Dynamic light scattering (DLS)

A commercialized spectrometer (Brookhaven Instruments Corporation, Holtsville, NY) equipped with a 100 mW solid-state laser (GXC-III, CNI, Changchun, China) operating at 532 nm was used to conduct dynamic light scattering experiments. Photon correlation measurements in self-beating mode were carried out at scattering angles of 30°, 60° and 90° using a BI-TurboCo Digital Correlator, where only the results in 90° were shown. The desired temperature was maintained by an external thermostat.

The normalized first-order electric field time correlation function $g^{(1)}(\tau)$ is related to the line width distribution $G(\Gamma)$ and the line width Γ by

$$g^{(1)}(\tau) = \int_0^\infty G(\Gamma)\exp(-\Gamma\tau)\ \mathrm{d}\Gamma \quad (1)$$

By using a Laplace inversion program, CONTIN, eqn (1) can be solved to obtain $G(\Gamma)$ and Γ, where Γ is related to the diffusion coefficient D and the scattering vector q by $\Gamma = Dq^2$. The apparent hydrodynamic radius $R_{h,app}$ can be obtained according to the Stokes–Einstein equation

$$R_{h,app} = k_B T/6\pi\eta D \quad (2)$$

where k_B, T, and η are the Boltzmann constant, absolute temperature, and viscosity of the solvent, respectively.

Time-resolved fluorescence quenching (TRFQ)

Pyrene was used as the fluorescence probe with dodecylpyridinium chloride ($C_{12}PyCl$) as the quencher. A desired amount of pyrene in ethanol was added to a test tube, followed by evaporation of the ethanol. Then a $C_{12}PyCl$-loaded DEAB/SDS/SC solution was added to the tube, which was vigorously stirred for 12 h. The concentration of pyrene was kept low enough (5×10^{-6} M) to prevent excimer formation. It has been shown in the literature that degassing neither affects the usefulness of eqn (3) nor provides a tangible gain in the fitting precision.[46] Therefore samples were not subjected to degassing. Pyrene fluorescence decay curves were monitored by an Edinburgh FLS920 time-resolved fluorescence spectrophotometer (excitation at 337 nm, emission at 385 nm, at 25 °C). The fluorescence decay curves were fitted to the Infelta–Tachiya equation

$$I(t) = I(0)\exp[-A_2 t - A_3(1 - \exp(-A_4 t))] \quad (3)$$

where $I(0)$ is the fluorescence intensity at $t = 0$, A_2 is the unquenched fluorescence decay rate constant, A_4 is the quenching rate constant, and A_3 represents the average number of quenchers per micelle. Assuming monodispersed micelles, one can relate the aggregation number N_{agg} to A_3 by

$$N_{agg} = CA_3/[Q] \quad (4)$$

where [Q] is the quencher concentration and C is the concentration of surfactant in micellar form.

Freeze-fracture transmission electron microscopy (FF-TEM)

Before the freezing procedure, samples were always incubated at a desired temperature. For the freezing procedure, a small amount of a sample was placed on a 0.1 mm thick copper disk and then covered with a second copper disk. The copper sandwich with the sample was frozen by plunging this sandwich into liquid propane which was cooled by liquid nitrogen. Aggregate structures were believed to be preserved and "solidified" by this procedure. Fracturing and replication were carried out in a freeze-fracture apparatus (BalzersBAF400, Germany) at −140 °C. Pt/C was deposited at an angle of 45° to shadow the replicas, and C was deposited at an angle of 90° to consolidate the replicas. The resulting replicas were examined using a JEM-100CX electron microscope.

Surface tension measurements

Surface tension measurements were conducted using the drop volume method at 25.0 °C. To provide constant ionic strength, all solutions were prepared with a buffer of 0.08 M NaBr. In addition, 0.01 M $Na_2B_4O_7$ and 0.01 M citric acid were used to keep the pH of solutions at 9.2 and 2.2, respectively. Since the ionic strength and [Na^+] were constant, the saturate adsorption amount of surfactant (Λ_∞) was calculated according to the Gibbs adsorption equation[47]

$$\Lambda_\infty = -\frac{1}{2.303RT}\frac{d\gamma}{d(\log C)} \quad (5)$$

where γ is the surface tension in mN m^{-1}, C represents the total concentration of surfactants, including DEAB, SDS, and SC, $d\gamma/d(\log C)$ is the slope of corresponding solid lines in Fig. S3 in the ESI†, T is the absolute temperature, and $R = 8.314$ J mol^{-1} K^{-1}. Then the average minimum area per surfactant molecule (A_{min}) in nm^2 is obtained from the saturate adsorption by

$$A_{min} = \frac{10^{18}}{N_A\Lambda_\infty} \quad (6)$$

where N_A is the Avogadro number. The average headgroup area of the DEAB/SDS/SC mixture, a, is approximately equal to the corresponding A_{min}.

Results and discussion

Effect of SC addition on DEAB/SDS vesicles at room temperature and neutral pH

This effect was reported in our previous work,[40] which will be briefly stated here. Before addition of SC, a DEAB/SDS (molar ratio 75/25, $C_{total} = 10$ mM) solution is dominated by vesicles. These DEAB/SDS vesicles do not show any response to temperature or pH variations, which is reasonable due to the lack of any responsive group in DEAB and SDS molecules.

Addition of SC at a low concentration (*ca.* >0.4 mM) to the DEAB/SDS solution is sufficient to transform the vesicles into micelles. Such a large influence of SC comes from two reasons: 1) the composition of DEAB/SDS (75/25) is close to a vesicle/micelle boundary, suggesting that the vesicles are ready to be turned into micelles; 2) the steric effect of SC is powerful owing to its large skeleton (~1.5 nm^2, Fig. 1). This remarkable effect of SC on DEAB/SDS vesicles is anticipated to benefit the present work.

Herein, we chose a DEAB/SDS/SC (molar ratio 75/25/4.5, $C_{total} = 10.45$ mM) solution, which is a micellar solution at 25 °C and pH 6.8, to investigate its responsive behaviors. The selected concentration of SC (0.45 mM) serves two purposes: bringing pronounced responsive abilities to the resultant aggregates and keeping [SC] itself as low as possible. Micelles in the solution were characterized by DLS and TRFQ measurements (Fig. 2). The DLS curve in Fig. 2a gives an $<R_{h,app}>$ of ~8 nm, which indicates that the micelles are likely to be short rods rather than spheres (the possibility of small vesicles is basically ruled out due to the absence of any vesicular structure in FF-TEM observations). According to the literature and our own experience, such micelles are hard to observe by negative stained- or FF-TEM. Thus we resorted to TRFQ measurements, where the fluorescence decaying curve (Fig. 2b) was fitted to eqn (3), giving an aggregation number (N_{agg}) of 370. Since N_{agg} values for spherical micelles are generally below ~100, the present value infers short rod-like micelles consistent with the DLS result. The following stimuli-responsive studies were performed in a DEAB/SDS/SC solution, in which the major aggregates were short rod-like micelles at 25 °C and pH 6.8.

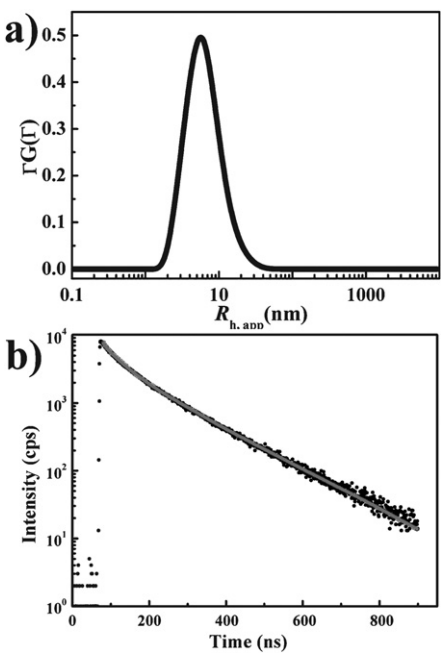

Fig. 2 The DEAB/SDS/SC (molar ratio 75/25/4.5, $C_{total} = 10.45$ mM) solution at 25 °C and pH 6.8. a) and b) DLS and TRFQ curves, respectively, where the solid line in b) is a fitting line.

Temperature-responsive behavior of the DEAB/SDS/SC solution

As the temperature was elevated from 25 to 80 °C (pH 6.8, unaltered), the colorless DEAB/SDS/SC solution turns into a bluish one (photographs in Fig. 3a). This bluish color is a manifestation of the Tyndall effect for large scatterers like vesicles in solution. Meanwhile the solution absorbance (or optical density) at 500 nm steadily increases from 0.002 to 0.045 (Fig. 3a, squares) due to a growth in aggregate size. An FF-TEM micrograph of the solution at 60 °C (Fig. 3b) demonstrates plenty of near-spherical structures with radii from 30–70 nm, confirming the existence of vesicles at a high temperature. This heating-induced micelle-to-vesicle transition (MVT) was further verified by DLS experiments (Fig. 4). Starting at 25 °C, a micellar peak with an $<R_h>$ of ~8 nm is predominant. At 35 °C, the micellar peak is still predominant with a broader size distribution. However, at 45 °C, a large vesicular peak with an $<R_h>$ of ~40 nm appears whereas the micellar peak shrinks dramatically. This suggests that a considerable number of micelles are converted into vesicles. At 60 °C, the micelle peak disappears, leaving the narrow vesicle peak with an $<R_h>$ of ~45 nm (in agreement with TEM observations), which indicates that micelles have been completely transformed into vesicles. In short, the DEAB/SDS/SC mixed solution exhibits a heating-induced MVT.

To examine the reversibility of this process, we carried out absorbance measurements during a decrease in temperature from 80 to 25 °C (Fig. 3a, circles). The solution absorbance decreased as expected, corresponding to a cooling-induced vesicle-to-micelle transition (VMT). It was further found that the two absorbance lines almost overlap with each other, indicating that this temperature-responsive transition between vesicles and micelles is fully reversible. Multiple heating/cooling cycles were also performed (Fig. 5), and an excellent reversibility was demonstrated. Once formed, vesicles exhibit time stability for at least two hours at a high temperature of 60 °C (see Fig. S1 in the ESI†).

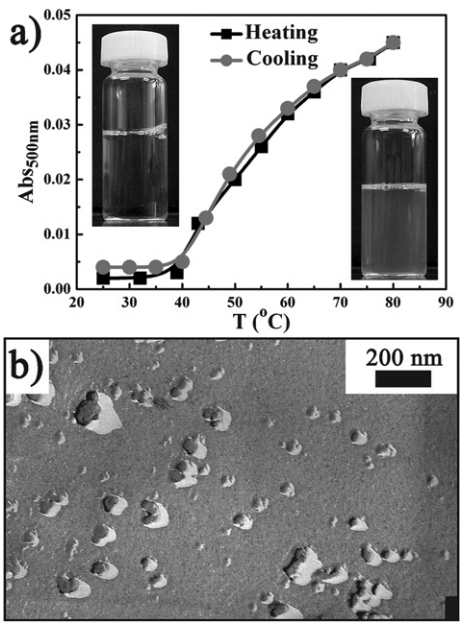

Fig. 3 The DEAB/SDS/SC (molar ratio 75/25/4.5, C_{total} = 10.45 mM) solution at constant pH 6.8 and various temperatures. a) Solution absorbance *versus* temperature: the squares for a heating process, the circles for a cooling process. Inserted photographs: left, a transparent solution at 25 °C; right, a bluish solution at 60 °C. b) An FF-TEM micrograph of the solution at 60 °C.

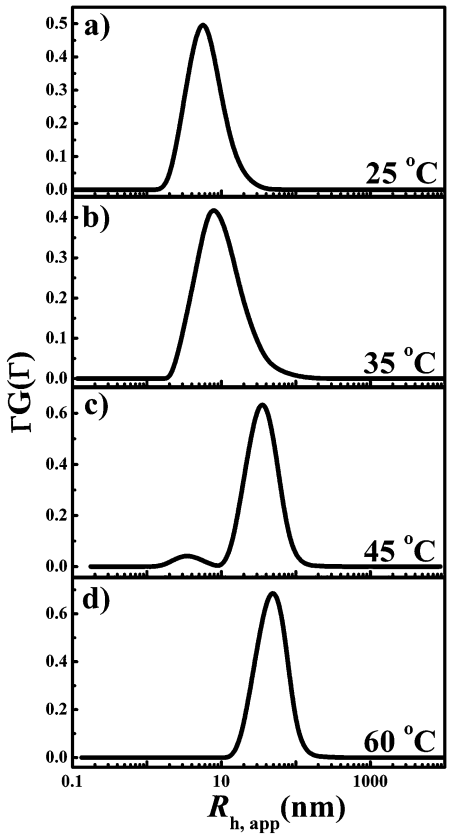

Fig. 4 The DEAB/SDS/SC (molar ratio 75/25/4.5, C_{total} = 10.45 mM) solution at constant pH 6.8 and various temperatures. a), b), c), and d) $<R_h>$ distributions at 25 °C, 35 °C, 45 °C, and 60 °C, respectively.

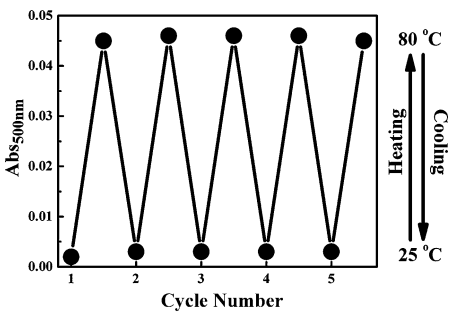

Fig. 5 The DEAB/SDS/SC (molar ratio 75/25/4.5, C_{total} = 10.45 mM) solution with constant pH 6.8 and various temperatures. The solution absorbance *versus* the heating/cooling cycle number.

pH-Responsive behavior of the DEAB/SDS/SC solution

In the case of pH decrease (a concentrated HBr solution was titrated into samples by a microsyringe, the temperature was kept at 25 °C), the DEAB/SDS/SC colorless solution turns bluish

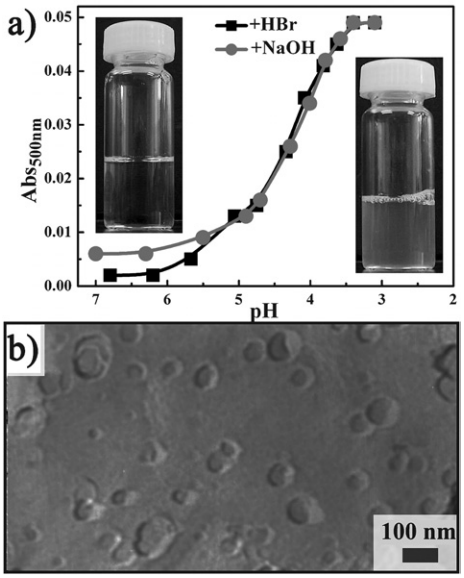

Fig. 6 The DEAB/SDS/SC (molar ratio 75/25/4.5, C_{total} = 10.45 mM) solution at a constant temperature of 25 °C and various pH values. a) Solution absorbance *versus* pH: the squares for an acidifying process, the circles for an alkalifying process. Inserted photographs: left, a transparent solution at pH 6.8; right, a bluish solution at pH 3.4. b) An FF-TEM micrograph of the solution at pH 3.4.

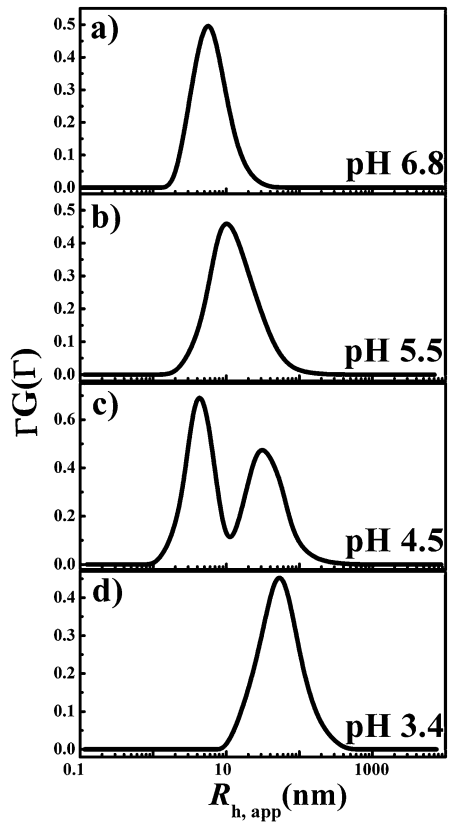

Fig. 7 The DEAB/SDS/SC (molar ratio 75/25/4.5, C_{total} = 10.45 mM) solution at a constant temperature of 25 °C and various pH values. a), b), c), and d) $<R_h>$ distributions at pH 6.8, 5.5, 4.5, and 3.4, respectively.

(photographs in Fig. 6a). At the same time, the absorbance of the solution rises slightly at first, followed by a drastic increase, and finally reaches a constant value (Fig. 6a, squares). The bluish appearance and absorbance increase with decreasing pH suggest the formation of large aggregates such as vesicles. The presence of vesicles at acidic pH was confirmed by lots of near-spherical structures with radii ranging from 25–60 nm in an FF-TEM micrograph (Fig. 6b). The pH value (4.2) for the most drastic variation in absorbance is close to the pK_a of SC (4.5, measured by pH titration) in this system, implying that this aggregate transition may arise from the protonization of SC (this will be discussed in the mechanism section). Moreover, DLS measurements were performed to follow the MVT process (Fig. 7). When the pH is reduced from 6.8 to 3.4, the micelle peak shrinks and vanishes, whereas the vesicle peak grows and dominates. For a sample with pH 3.4, micelles are completely converted into vesicles. According to the above results, the DEAB/SDS/SC solution displays an acidic pH-induced MVT.

The reversibility of this acidic pH-induced MVT was tested by absorbance measurements. A concentrated NaOH solution was titrated into the acidic DEAB/SDS/SC solution to neutralize the HBr and to increase the pH from 3.4 to 6.8. The absorbance decreased as expected (Fig. 6a, circles), suggesting an alkali pH-induced VMT. However, the mismatch of absorbance lines at high pH values (*ca.* >5) indicates that this pH-responsive transition is only reversible to some extent. Correspondingly, more pH cycles gives rise to higher absorbance values in comparison to the original values (Fig. 8a), which may be a result of the excess NaBr produced by the pH cycles. The excess NaBr will screen the charge of the ionic surfactant headgroups, favoring low-curved aggregate-like vesicles. For the solution with pH 6.8 at the third cycle, a relatively broad micellar peak and a little vesicular peak are observed in its DLS curve (Fig. 8b), suggesting that the appearance of a small number of vesicles may be responsible for the absorbance increase. Once formed, vesicles exhibit time stability for at least two weeks at an acidic pH of 3.4 (see Fig. S2 in the ESI†).

In addition, it can be expected that vesicles are the predominant aggregates at both high temperature (60 °C) and acidic pH (3.4), because vesicles dominate the solution at either one of the two conditions. This expectation is confirmed by the results of DLS and FF-TEM (Fig. 9). Combining the above temperature- and pH-responsive behaviors of the DEAB/SDS/SC solution, we

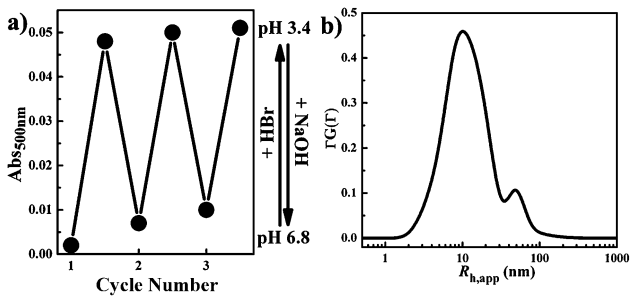

Fig. 8 The DEAB/SDS/SC (molar ratio 75/25/4.5, C_{total} = 10.45 mM) solution at a constant temperature of 25 °C and various pH values. a) Solution absorbance *versus* the acidifying/alkalifying cycle number. b) An $<R_h>$ distribution of the solution with pH 6.8 at the third cycle.

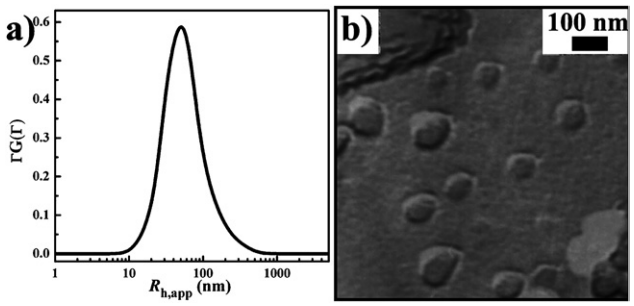

Fig. 9 The DEAB/SDS/SC (molar ratio 75/25/4.5, C_{total} = 10.45 mM) solution at 60 °C and pH 3.4. a) and b), a DLS curve and an FF-TEM micrograph, respectively.

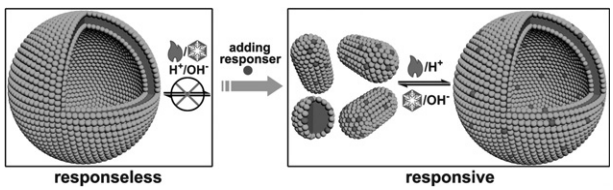

Fig. 10 The addition of a responser (SC) endows responseless catanionic surfactant vesicles with temperature- and pH-responsive abilities.

can draw the following conclusion: after the addition of a small amount of SC, the responseless or stimuli-inert DEAB/SDS vesicles are converted into temperature- and pH-responsive aggregates that undergo the MVTs as induced by heating or acidifying and the VMTs as induced by cooling or alkalifying (Fig. 10). This DEAB/SDS/SC system establishes a successful instance for the proposed noncovalent strategy, where a simple introduction of a responser endows catanionic surfactant vesicles with responsive abilities.

Mechanism for the temperature- and pH-responsive behavior

The geometry rule[48] has been widely and successfully used to explain surfactant aggregate transitions where p is the packing parameter: $0 < p < 1/2$ for micelles and $1/2 < p < 1$ for vesicles. P is defined as v/al, where v is the surfactant tail volume, l the tail length, and a the headgroup area (for mixed surfactant systems, they are average values). A connection between features in the SC molecular structure and the geometry rule may help us to understand the observed responsive behavior. At room temperature and neutral pH, SC molecules in the mixed DEAB/SDS/SC aggregates are of an orientation[49,50] parallel to the surface with its polar and nonpolar faces towards the water and hydrocarbon region, respectively. Such parallel arrangement of SC greatly increases the average a value (0.26 nm^2 for the DEAB/SDS mixture and 0.56 nm^2 for the DEAB/SDS/SC mixture) and consequently decreases p, leading to an SC-induced VMT (Fig. 11a and 11b).[40]

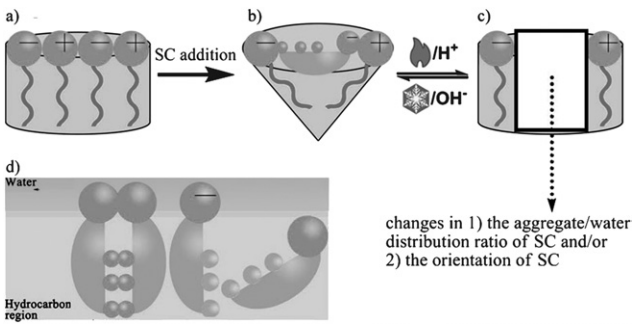

Fig. 11 Molecular packing for a) DEAB/SDS and b) DEAB/SDS/SC mixtures at room temperature and neutral pH, and c) upon changing the temperature or pH. d) Three hypothesized nonparallel orientations.

For a given amount of SC, its effect on the aggregates depends on its aggregate/water distribution ratio and its orientation in the aggregates, both of which will be affected by temperature or pH variations due to the presence of temperature-responsive hydroxyl groups and pH-responsive carboxylate group in SC molecules (Fig. 11c). Regarding how temperature or pH will influence the distribution ratio and orientation of SC in our case, it is hard to obtain direct and conclusive results for such a low concentration of SC (0.45 mM). More powerful NMR diffusion and relaxation techniques could shed more light on the distribution ratio and orientation of SC, respectively. At the present stage, only preliminary discussion and speculation are presented.

The aggregate/water distribution ratio of a surfactant is generally closely related to its critical micelle concentration (CMC): a higher CMC corresponds to a lower distribution ratio. It was reported that the CMC of SC increases upon heating[51] (10 mM for 25 °C and 15.5 mM for 70 °C) and rises by a remarkable amount upon alkalifying[52] (1.99 mM in 50 mM NaCl and 6.03 mM in 45 mM NaCl + 5 mM NaOH). For the DEAB/SDS/SC mixture, the temperature–CMC data suggests that some SC molecules will move from the aggregates to water upon heating, partially "undoing" the original SC-induced VMT at room temperature and contributing to the observed heating-induced MVT. The pH-CMC data suggests that more SC molecules will be incorporated into the aggregates upon acidifying, which would even enhance the original SC-induced VMT if the orientation of SC is not changed. Since an acidic pH-induced VMT is observed, changes in the SC orientation may be involved for acidifying process.

The parallel orientation of SC (at room temperature and neutral pH, Fig. 11b) possesses the maximum apparent headgroup area (~1.5 nm^2), which means that any nonparallel orientations are of smaller apparent headgroup areas. The parallel orientation arises out of the unique facial amphiphility of SC. The polar face of SC, however, will (partially) lose its hydrophilic nature by dehydration of the hydroxyl groups and/or deionization of the carboxylate group. In such cases, SC may adopt nonparallel orientations. Three hypothesized nonparallel modes are illustrated in Fig. 11d as examples: SC may dimerize through intermolecular hydrogen bonds, embed its steroid frame and dehydrated hydroxyl groups into the hydrocarbon region, or simply reside in the hydrocarbon region without special orientation. If a parallel-to-nonparallel orientation transition occurs, a decrease in the average headgroup area a is expected. For the DEAB/SDS/SC mixture, a decrease of a from 0.56 nm^2 (pH 9.2, fully ionized SC) to 0.35 nm^2 (pH 2.2, fully protonized SC) is determined by surface tension curves (Fig. S3 in the ESI†). This a decrease may come from a parallel-to-nonparallel orientation transition and contribute to the observed acidifying-induced MVT. At acidic pH, the dimerization mode, compared to the

other two modes, is more likely to be favored by SC, which is supported by dimerization or tetramerization of neutral cholate derivatives.[53,54] A decrease of a at high temperature is not yet evidenced because surface tension measurements suffer from rapid evaporation of water at high temperature. However, a parallel-to-nonparallel orientation transition and a decrease of a as induced by heating cannot be ruled out at the present stage.

Although the mechanism for the responsive behavior is not fully understood, a preliminary explanation is accessed on the basis of the above discussion. An increase in the CMC of SC promotes the heating-induced MVT, which might also be contributed by a transition in SC orientation. The deionization of SC and the consequent parallel-to-nonparallel orientation transition are responsible for the acidifying-induced MVT.

Extending the strategy to other catanionic surfactant vesicles

The required amounts of SC were added to DE_2MAB/SDS, DPAB/SDS, and DTAB/SDBS vesicular solutions (for abbreviations, see Materials section), respectively, leading to VMTs as expected. These resultant SC-loaded mixed micellar solutions were then subjected to temperature and pH variations, for which the corresponding absorbance curves are plotted in Fig. 12. When the temperature is elevated, the absorbance increases for the DE_2MAB/SDS/SC and DPAB/SDS/SC mixed solutions but remains unchanged (still as clear as water) for the DTAB/SDBS/SC solution (Fig. 12a). It is suggested that the former two systems exhibit heating-induced MVTs while the latter one does not. This discrepancy can be attributed to the different temperature-dependence of the original vesicular solutions: upon heating, the DE_2MAB/SDS and DPAB/SDS vesicular solutions keep their absorbance constant as the DEAB/SDS solution does, whereas the DTAB/SDBS vesicular solution shows a decrease in absorbance (see Fig. S4 in the ESI†), which will counteract the effect of the added SC. As for an acidifying process, all the three SC-loaded systems undergo MVTs as suggested by the absorbance increase (Fig. 12b). Therefore, the present responsive ability-endowing noncovalent strategy is valid for different kinds of catanionic surfactant vesicles (although not every kind). Moreover, because catanionic surfactant systems can form various self-assemble aggregates, other transitions (*e.g.*, spherical/worm-like micelles, vesicles/tubes, and vesicles/lamellae) are potentially accessible by this strategy.

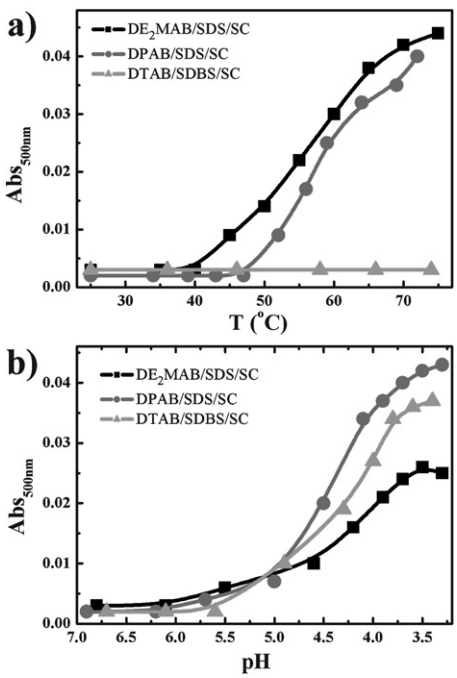

Fig. 12 a) Temperature-responsive and b) pH-responsive behavior of three SC-loaded systems: DE_2MAB/SDS/SC (molar ratio 80/20/5, C_{total} = 10.5 mM), DPAB/SDS/SC (molar ratio 75/25/3, C_{total} = 10.3 mM), and DTAB/SDBS/SC (molar ratio 80/20/27, C_{total} = 12.7 mM).

Conclusions and the responsive ability-endowing noncovalent strategy

Responseless catanionic surfactant DEAB/SDS vesicles are endowed with dual responsive abilities by the simple introduction of the responser, SC, at a low SC/surfactant molar ratio of 0.045. The resultant DEAB/SDS/SC aggregates undergo reversible transitions between vesicles and micelles in response to temperature or pH variations, which is attributed to the temperature-responsive hydroxyl groups and pH-responsive carboxylate group of SC. The temperature- and pH-responsive MVT and VMT may be attractive for protein reconstitutions, for gene delivery, and particularly for controlled-release of drugs, because a sick tissue or organ corresponds to an abnormal temperature and/or pH. Additional features of this DEAB/SDS/SC system, including the low concentration, biocompatibility, and commercial availability of SC as well as the reversibility of the transitions, may benefit its applications.

This work presents an illustrative example of the responsive ability-endowing noncovalent strategy. This strategy sidesteps difficult syntheses and alternatively relies on using the noncovalent combination of a catanionic surfactant mixture and a responser. Desired catanionic surfactant aggregates that are ready to be transformed can be obtained by careful selection of surfactant compositions, which is a trick of this strategy. As for the responser, it requires a molecule that bears responsive groups and can be incorporated into the aggregates (as long as it is somewhat hydrophobic). This requirement can be easily met by abundant commercially available hydrotropes, dyes, and other molecules, such as light-responsive cinnamic acid, redox-responsive ferrocene carboxylic acid, and pH-responsive malachite green. Meanwhile, the endowing of multiple responsive abilities is more feasible by the noncovalent strategy than by covalent syntheses. To conclude, this responsive ability-endowing noncovalent strategy can provide a versatile and economical method to fabricate stimuli-responsive and "smart" self-assemblies, which may open a new vista in constructing multi-functional aggregates.

Acknowledgements

This work was supported by the National Natural Science Foundation of China and the National Basic Research Program of China (Grant No. 2007CB936201). We thank the Center for Biological Electron Microscopy and the Institute of Biophysics for electron microscopy work and Shufeng Sun for making TEM samples. We thank Na Du for her help in DLS measurements.

References

1 J. Fendler, *Membrane Mimetic Chemistry*, John Wiley & Sons, New York, 1983.
2 *Vesicles*, ed. M. Rosoff, Marcel Dekker, New York, 1996.
3 M. M. Hanczyc, S. M. Fujikawa and J. W. Szostak, *Science*, 2003, **302**, 618.
4 A. B. Shaul, W. M. Gelbart and D. Roux, *Micelles, Membranes, Microemulsions and Monolayers*, Springer, Berlin, 1995.
5 P. J. Reeves, J. Hwa and H. G. Khorana, *Proc. Natl. Acad. Sci. U. S. A.*, 1999, **96**, 1927.
6 D. T. McQuade, M. A. Quinn, S. M. Yu, A. S. Polans, M. P. Krebs and S. H. Gellman, *Angew. Chem., Int. Ed.*, 2000, **39**, 758.
7 A. M. Seddon, P. Curnow and P. J. Booth, *Biochim. Biophys. Acta*, 2004, **1666**, 105.
8 F. M. Winnik and D. G. Whitten, *Langmuir*, 2007, **23**, 1.
9 R. J. Mart, Rachel D. Osborne, M. M. Stevens and R. V. Ulijn, *Soft Matter*, 2006, **2**, 822.
10 S. Ahn, R. M. Kasi, S.-C. Kim, N. Sharma and Y. Zhou, *Soft Matter*, 2008, **4**, 1151.
11 P. F. Kiser, G. Wilson and D. Needham, *Nature*, 1996, **394**, 459.
12 N. Morimoto, N. Ogino, T. Narita, S. Kitamura and K. Akiyoshi, *J. Am. Chem. Soc.*, 2007, **129**, 458.
13 B. Carion-Taravella, S. Lesieur, M. Ollivon and J. Chopineau, *J. Am. Chem. Soc.*, 1998, **120**, 10588.
14 M. Johnsson, A. Wagenaar and J. B. F. N. Engberts, *J. Am. Chem. Soc.*, 2003, **125**, 757.
15 C. Z. Wang, Q. Gao and J. B. Huang, *Langmuir*, 2003, **19**, 3757.
16 S. J. Ryhanen, V. M. J. Saily, M. J. Parry, P. Luciani, G. Mancini, J.-M. I. Alakoskela and P. K. J. Kinnunen, *J. Am. Chem. Soc.*, 2006, **128**, 8659.
17 J. C. Medina, I. Gay, Z. Chen, L. Echegoyen and G. W. Gokel, *J. Am. Chem. Soc.*, 1991, **113**, 365.
18 Y. Kakizawa, H. Sakai, K. Nishiyama and M. Abe, *Langmuir*, 1996, **12**, 921.
19 K. Monserrat, M. Gratzel and P. Tundolb, *J. Am. Chem. Soc.*, 1980, **102**, 5521.
20 Y. Wang, N. Ma, Z. Wang and X. Zhang, *Angew. Chem., Int. Ed.*, 2007, **46**, 2823.
21 S. M. Lee, H. Chen, C. M. Dettmer, T. V. O'Halloran and S. T. Nguyen, *J. Am. Chem. Soc.*, 2007, **129**, 15096.
22 H. Okabe, S. Kamagami, H. Kainose, Y. Ishigami and Yutaka, *Chem. Express*, 1991, **6**, 315.
23 C. Z. Wang, J. B. Huang and B. Y. Zhu, *Langmuir*, 2003, **19**, 7676.
24 T. A. Waggoner, J. A. Last, P. G. Kotula and D. Y. Sasaki, *J. Am. Chem. Soc.*, 2001, **123**, 496.
25 M. Nobuyuki, O. Naruhito, N. Tadashi, K. Shinichi and A. Kazunari, *J. Am. Chem. Soc.*, 2007, **129**, 458.
26 D. Otten, L. Lobbecke and K. Beyer, *Biophys. J.*, 1995, **68**, 584.
27 R. T. Buwalda, M. C. A. Stuart and J. B. F. N. Engberts, *Langmuir*, 2000, **16**, 6780.
28 T. S. Davies, A. M. Ketner and S. R. Raghavan, *J. Am. Chem. Soc.*, 2006, **128**, 6669.
29 A. M. Ketner, R. Kumar, T. S. Davies, P. W. Elder and S. R. Raghavan, *J. Am. Chem. Soc.*, 2007, **129**, 1553.
30 E. W. Kaler, A. K. Murthy, B. E. Rodriguez and J. A. N. Zasadzinski, *Science*, 1989, **245**, 1371.
31 J. Hao and H. Hoffmann, *Curr. Opin. Colloid Interface Sci.*, 2004, **9**, 279.
32 C. Tondre and C. Caillet, *Adv. Colloid Interface Sci.*, 2001, **93**, 115.
33 M. Dubios, B. Deme, T. Gulik-Krzywicki, J.-C. Dedieu, C. Vautrin, S. Desert, E. Perez and T. Zemb, *Nature*, 2001, **411**, 672.
34 T. Zemb, M. Dubios, B. Deme and T. Gulik-Krzywicki, *Science*, 1999, **283**, 816.
35 A. X. Song, S. L. Dong, X. F. Jia, J. C. Hao, W. M. Liu and T. B. Liu, *Angew. Chem., Int. Ed.*, 2005, **44**, 4018.
36 A. Gonzalez-Perez, M. Schmutz, G. Waton, M. J. Romero and M. P. Krafft, *J. Am. Chem. Soc.*, 2007, **129**, 756.
37 T. Lu, F. Han, Z. C. Li, J. B. Huang and H. L. Fu, *Langmuir*, 2006, **22**, 2045.
38 Y. Yan, W. Xiong, X. X. Li, T. Lu, J. B. Huang, Z. C. Li and H. L. Fu, *J. Phys. Chem. B*, 2007, **111**, 2225.
39 J.-P. Douliez, *J. Am. Chem. Soc.*, 2005, **127**, 15694.
40 L. X. Jiang, K. Wang, M. L. Deng, Y. L. Wang and J. B. Huang, *Langmuir*, 2008, **24**, 4600.
41 H. Q. Yin, S. Lei, S. B. Zhu, J. B. Huang and J. P. Ye, *Chem. Eur. J.*, 2006, **12**, 2825.
42 M. Mao, J. B. Huang, B. Y. Zhu, H. Q. Yin and H. L. Fu, *Langmuir*, 2002, **18**, 3380.
43 A. F. Hofmann and D. M. Small, *Annu. Rev. Med.*, 1967, **18**, 333.
44 M. C. Carey and D. M. Small, *Am. J. Med.*, 1970, **49**, 590.
45 S. H. Tung, Y. E. Huang and S. R. Raghavan, *J. Am. Chem. Soc.*, 2006, **128**, 5751.
46 J. Singh, Z. Unlu, R. Ranganathan and P. Griffiths, *J. Phys. Chem. B*, 2008, **112**, 3997.
47 R. Aveyard and D. A. Haydon, *An Introduction to the Principles of Surface Chemistry*, Cambridge University Press, London, 1973.
48 J. N. Israelachvili, D. J. Mitchell and B. W. Ninham, *J. Chem. Soc., Faraday Trans. 2*, 1976, **72**, 1525.
49 J. Ulmius, G. Lindblom, H. Wennerstrom, L.-B. Johansson, K. Fontell, O. Soderman and G. Arvidson, *Biochemistry*, 1982, **21**, 1553.
50 R. P. Hjelm, Jr., P. Thiyagarajan and H. Alkan-Onyuksel, *J. Phys. Chem.*, 1992, **96**, 8653.
51 P. Garidel, A. Hildebrand, R. Neubert and A. Blume, *Langmuir*, 2000, **16**, 5267.
52 M. Swanson-Vethamuthu, M. Almgren, P. Hansson and J. Zhao, *Langmuir*, 1996, **12**, 2186.
53 V. Janout, M. Lanier and S. L. Regen, *J. Am. Chem. Soc.*, 2001, **123**, 5401.
54 K. Ariga, Y. Terasaka, D. Sakai, H. Tsuji and J. Kikuchi, *J. Am. Chem. Soc.*, 2000, **122**, 7835.